



ISSN: 0976-3031

Available Online at <http://www.recentscientific.com>

CODEN: IJRSFP (USA)

*International Journal of Recent Scientific Research*  
Vol. 8, Issue, 11, pp. 21701-21707, November, 2017

**International Journal of  
Recent Scientific  
Research**

DOI: 10.24327/IJRSR

## Research Article

### MODELING AND VALIDATION OF GATIMAAN EXPRESS WITH VI-RAIL

**Prabin Kumar Jha and Gokhale S.S**

Department of Mechanical-Mechatronics Engineering the LNM Institute of Information Technology  
Rupa Ki Nangal, Post Sumel, via Jamdoli Jaipur-302031 India

DOI: <http://dx.doi.org/10.24327/ijrsr.2017.0811.1123>

#### ARTICLE INFO

##### Article History:

Received 06<sup>th</sup> August, 2017  
Received in revised form 14<sup>th</sup>  
September, 2017  
Accepted 23<sup>rd</sup> October, 2017  
Published online 28<sup>th</sup> November, 2017

##### Key Words:

Derailment coefficients, Lateral Force,  
Primary and Secondary Suspensions,  
Vertical Forces, VI-Rail

#### ABSTRACT

Indian railways has the fourth largest network in the world. Short or medium distance travel by air causes considerable pollution per passenger. As an alternative objective of reducing environment pollution, superfast train option is studied. As a first step, speeding up of trains with existing infrastructure and same rail tracks is explored. The distance of 200 km between New Delhi and Agra cantonment is covered in 105 minutes with an average speed of 160 kmph. A 3D model of complete train is developed in VI Rail and results are compared with measured data obtained from Research Design and Standards Organization (RDSO) of Indian Railways. Present study analyzes translatory motion in terms of lateral and vertical accelerations which depend on primary and secondary suspension. The values of primary and secondary suspensions are changed in the 12<sup>th</sup> car body, 6<sup>th</sup> car body and 1<sup>st</sup> car body to study the derailment. The critical speed at which Gatimaan Express model can be derailed, is determined.

**Copyright © Prabin Kumar Jha and Gokhale S.S, 2017**, this is an open-access article distributed under the terms of the Creative Commons Attribution License, which permits unrestricted use, distribution and reproduction in any medium, provided the original work is properly cited.

#### INTRODUCTION

Many researchers have studied the dynamics behaviour of rail vehicle in various softwares such VI-Rail, Vampire and Simpack rail and Matlab/Simulink etc. Arvind *et al.* [1] compared the ride index of IRY-IR20 and LHB bogies at different speeds (60 kmph, 120 kmph and 180 kmph) in ADAMS/Rail and found the lateral ride index lower in LHB bogie than in IR20 bogie whereas the vertical ride index was slightly higher in LHB bogie than in the IR20 bogie. Herrero [2] studied a 50 degree of freedom of rail vehicle model in Simpack Rail. He compared the ride comfort, safety and wear dynamics with the measured data. Further, he optimized the primary suspension parameters and the results were taken into account for the performance improvement of existing primary suspension. Ellermann and Jesussek [3] applied fault detection and isolation methods (FDI) to nonlinear suspension system of a railway vehicle. An optimal and robust filter was designed to detect the failure of suspension system. They also studied the fault in anti-yaw damper. Melnik and Sowiski [4] developed online motoring of suspension. It was based on the suspension acceleration signature. They performed the experiment on a wagon with a damaged suspension and observed that the model was damage sensitive. Dwyer *et al.* [5] made a model to predict the wear on the wheels of a railway vehicle. They had carried out a test on a twin disc wheel to get coefficient of wear.

Further, it was incorporated in ADAMS/Rail model to study the performance of wheel and rail dynamics. The model was utilized to predict the wear of the wheel. Liu *et al.* [6] reported that about 30% of the derailments were caused by suspension defects based on data provided by Federal Railroad Administration (FRA), USA during the period from 2001 to 2010. Ju [7] substantiated that the damage in the primary suspension is one of the prime causes of train derailment rather than the damage in the secondary suspension. This is due to the direct impact of primary suspension on the wheel/rail contact dynamics. Lu and Hecht [8] developed a double Decker passenger vehicle with bogie PW200 in ADAMS/Rail and compared the simulated results of suspension performance with the measured field data and further optimized the bogie suspension parameters to improve vehicle dynamics on the curve track.

Montiglio and Stefanini [9] studied the semi active lateral suspension of a tilting train (an ability of train to tilt its coach inwards on curve) in ADAMS/Rail and co-simulation was carried out with Matlab/Simulink. The results were compared with the passive suspension performance and were found satisfactory. Thomas [10] designed a 3D model of vehicle for lateral dynamics at high speed because of influence of the track curves and track irregularities. He observed that vehicle stability was more crucial because of encountering of

\*Corresponding author: **Prabin Kumar Jha**

Mechanical-Mechatronics Engineering Department, the LNM Institute of Information Technology Rupa Ki Nangal, Post-Sumel, via Jamdoli, Jaipur

centrifugal force on the curve track than on the tangential track. Moody [11] analyzed the critical speed of rail vehicle on the curve as well as straight tracks. He investigated the behaviour of torques due to centrifugal force and weight acting at the wheel and rail contact point on the curve track. The unbalancing of these two torques created the train derailment.

Sezer *et al.* [12] developed a 54 DoF railway vehicle model in Matlab/Simulink. They studied the dynamic response of the model due to the different rail irregularities. Polach [13] studied the dynamic behaviour of wheel-rail interaction on adhesion limit which had a large longitudinal creep. He simulated the model with different real wheel and rail contact conditions. He noticed that the effect of vehicle speed, longitudinal, lateral and spin creep and shape of the contact ellipse during the simulation. The method was validated by comparisons with the measurements and was found satisfactory. Y. Tsai *et al.* [14] designed a 28 DoF of dynamic model in Matlab/Simulink and compared stability performances with the test data of vehicle operated by Taipei Rapid Transit Corporation. The result was satisfactory. They considered random inputs of various types of track irregularities in the model. Meisinger [15] developed a linear model based on creep-controlled wheelset. He calculated the root-locus for quasi-statical during the curving. The hunting stability behaviour and curving capability was investigated for different feedback of the creep for both wheels. He noticed the instability of wheelset dynamics at the speed of 75m/s.

**Scope of Research work**

From the literature survey, it can be concluded that various models have been developed in multi-body simulation softwares as well as computing software to study the ride comfort, wear dynamics, nonlinear characteristics of suspension, the critical speed of the train at the curve track and hunting behaviour. But the present work includes the simulation of Gatimaan Express model and its validation with the measured field data provided by Testing Directorate, RDSO. The derailment of the model due to high speed is studied. In addition to these, the derailment of model due to failure of primary and secondary suspensions are studied.

**Development of Gatimaan Express model in VI-Rail**

Gatimaan Express model is having mainly three subsystems namely; car body, LHB bogie and wheel sets. The car body is modeled in Solid works as per the given dimensions from the maintenance manual of LHB coach [16]. The developed model is shown in Figure 1.

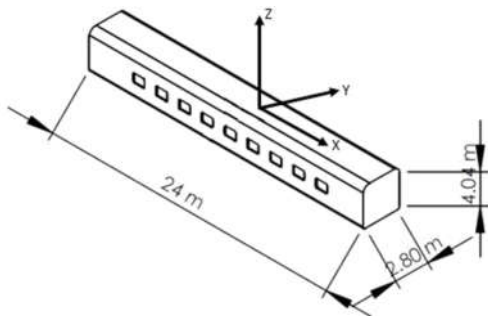


Figure 1 Dimension of Gatimaan Express model

The LHB bogie consists of primary suspensions, primary dampers, secondary suspensions, secondary dampers, yaw dampers, lateral damper as given in Table 1.

Table 1 Main components of LHB bogie [16]

S.No.	Name of component	Quantity
1.	Secondary spring	2
2.	Secondary damper	2
3.	Primary spring	4
4.	Primary damper	4
5.	Secondary lateral damper	1
6.	Yaw damper	2

The VI-Rail model of bogie is further modified as per LHB bogie as shown in Figure 2. Following assumptions are made for the study:

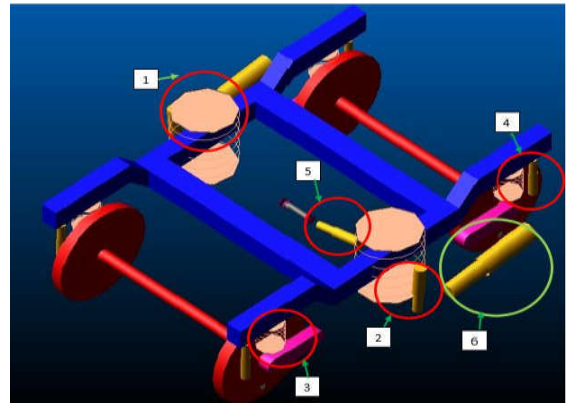


Figure 2 LHB Bogie model in VI Rail

- There is no crack on wheel and rail
- There is no wear on wheel and rail
- Straight and curve with transition tracks is considered
- Coupler of each coach has same characteristics
- Point mass is considered for all coaches
- Coefficient of friction between wheel and rail is constant
- Suspension of each coach has same characteristics
- Smooth wheel and rail is presumed
- There is no rail joint
- There is no corrugation on rail

The field data of lateral and vertical accelerations of loco, one generator van, one second class A/C chair car and one executive class A/C chair car of Gatimaan Express during

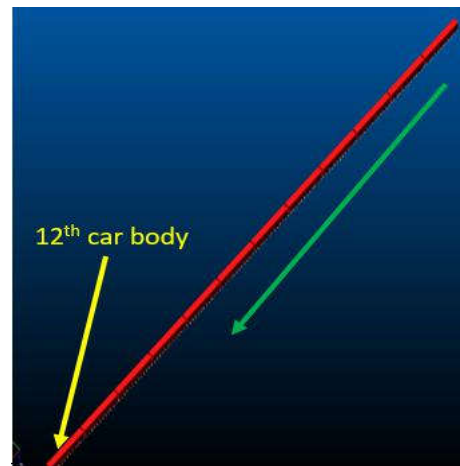


Figure 3 A Complete Gatimaan Express model in VI-Rail.

trail run from New Delhi to Agra Cantonment was recorded for the distance of 17 km. The measuring instrument with accelerometer sensors was equipped on the floor level over the bogie pivot of respective car bodies. These accelerations with speed of train were recorded by RDSO in real time by using LabView of National Instruments at the sampling rate of 100 samples per second and low pass fifth order Butterworth filter of 10 Hz. The car body model is imported in VI-Rail. As the Gatimaan Express has 12 coaches so the model is made for 12 car bodies with the help of couplers in VI-Rail as shown in Figure 3.

**Simulation Setting for Gatimaan Express model in VI-Rail**

The track geometry from Agra Cantonment to Palwal and measured velocity are incorporated. The signature of measured velocity is shown in Figure 4.

```

$-----
IRREGULARITIES
(IRREGULARITIES)
TYPE = 'ANALYTIC PSD'
FORMAT = 'PSD_1'
INTERPOLATION = 'SPLINE'
SCALE = 1.0
DATA STEP = 0.2
INACTIVE_LENGTH = 2.0
ACTIVE_LENGTH = 4217.0
FREQUENCY_TERMS = 200.0
PSD_OC = 0.8246
PSD_OR = 0.0206
PSD_OS = 0.438
PSD_AV = 4.032E-07
PSD_RA = 2.119E-07
PSD_L1 = 2.0
PSD_L2 = 20000.0
LAT_ACTIVE = 'YES'
VER_ACTIVE = 'YES'
ROLL_ACTIVE = 'YES'
$-----
HORIZONTAL PATH
(HORIZONTAL_PATH)
{horizontal_s curvature kink}
0.0 0.0 0.0
500.0 0.0 0.0
830.0 -0.0011 0.0
1747.0 0.0 0.0
2187.0 0.0013 0.0
3677.0 0.0 0.0
4217.0 -0.0014 0.0
$-----
VERTICAL PATH
(VERTICAL_PATH)
{vertical_s coordinate}
0.0 0.0
4217.0 0.0
    
```

Figure 4 Track profile in VI-Rail.

The track length 4.217 km is taken into account for simulation as shown in Figure 5.

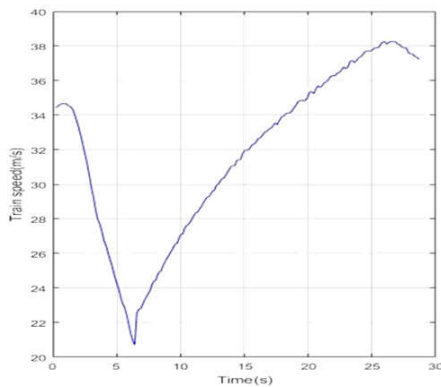


Figure 5 Measured Velocity(m/s) of Gatimaan Express during test run.

The s1002 in VI-Rail is considered as wheel property file. It is basically UIC60 rail which has 60kg/m, conicity of 1:40 and is used for high speed train. The conicity allows wheel to steer on the curve. Train model on S-shape track is shown in Figure 6. The PSD is calculated for rail irregularities in VI-Rail. It is a type of spatial frequency of the rail perturbations. The vertical ( $i_{r_{zz}}$ ), lateral ( $i_{r_{yy}}$ ) and cant ( $i\phi_{sec}$ ) PSDs are given in the following equations [17].

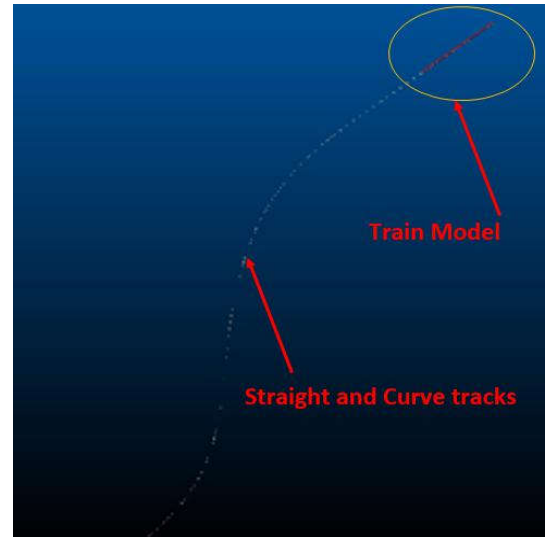


Figure 6 Gatimaan Express model on S-shape track.

$$i_{r_{zz}} = \frac{A_v \omega_c^2}{(\omega^2 + \omega_c^2)(\omega^2 + \omega_r^2)}, \tag{1}$$

$$i_{r_{yy}} = \frac{A_a \omega_c^2}{(\omega^2 + \omega_c^2)(\omega^2 + \omega_r^2)}, \tag{2}$$

$$i\phi_{sec} = \frac{1}{a} \frac{A_v \omega_c^2}{(\omega^2 + \omega_c^2)(\omega^2 + \omega_s^2)(\omega^2 + \omega_r^2)}, \tag{3}$$

Where, A, a,  $A_v$ ,  $\omega_c$ ,  $\omega$ ,  $\omega_s$ ,  $\omega_r$  are quality of rail, half of track width, circular frequency for curve track, circular frequency, circular frequency for curve track, circular frequency for straight track and circular frequency for rail.

Stabilized Index-2 (SI2) with integrator GSTIFF scheme is implemented to solve a set of coupled differential and algebraic equations. These equations are stiff when they have both high and low eigen value frequencies. Thus, stiff differential equations require stiff integration methods to solve the problem efficiently and accurately. It is a SI2 method to provide better error control over the velocity and acceleration solving problems. The HMAX 2.8875e-3 (maximum time step, calculated as given in [17]) are comprised of a solver setting of VI-Rail. The HMAX 1.6129e-3 is taken for high speed (223 kmph) simulation.

```

$-----MOT_HEADER
[MOT_HEADER]
FILE_TYPE = 'Preload Analysis'
FILE_VERSION = 1.0
FILE_FORMAT = 'ASCII'
$-----UNITS
[UNITS]
LENGTH = 'meter'
ANGLE = 'degree'
FORCE = 'newton'
MASS = 'kg'
TIME = 'second'
$-----SUSPENSION_ELEMENT
[SUSPENSION_ELEMENT]
%SUSPENSION_ELEMENT = 144
SUSPENSION_ELEMENT_1 = 'NDLS_AGRA_12coaches.F_front_bogie_01.uel_front_ps'
T_PRELOAD_1 = 1.8E+06
SUSPENSION_ELEMENT_2 = 'NDLS_AGRA_12coaches.F_front_bogie_01.uel_rear_ps'
T_PRELOAD_2 = 1.8E+06
SUSPENSION_ELEMENT_3 = 'NDLS_AGRA_12coaches.F_front_bogie_01.uel_rear_ps'
T_PRELOAD_3 = -1.8E+06
SUSPENSION_ELEMENT_4 = 'NDLS_AGRA_12coaches.F_front_bogie_01.uel_rear_ps'
T_PRELOAD_4 = 7.1E+05
SUSPENSION_ELEMENT_5 = 'NDLS_AGRA_12coaches.F_front_bogie_01.uel_ss'
T_PRELOAD_5 = 7.2E+05
SUSPENSION_ELEMENT_6 = 'NDLS_AGRA_12coaches.F_front_bogie_01.uel_ss'
T_PRELOAD_6 = 7.2E+05
SUSPENSION_ELEMENT_7 = 'NDLS_AGRA_12coaches.F_front_bogie_02.uel_front_ps'
T_PRELOAD_7 = 1.4E+06
SUSPENSION_ELEMENT_8 = 'NDLS_AGRA_12coaches.F_front_bogie_02.uel_rear_ps'
T_PRELOAD_8 = 1.4E+06
SUSPENSION_ELEMENT_9 = 'NDLS_AGRA_12coaches.F_front_bogie_02.uel_rear_ps'
T_PRELOAD_9 = -8.3E+05
SUSPENSION_ELEMENT_10 = 'NDLS_AGRA_12coaches.F_front_bogie_02.uel_rear_ps'
T_PRELOAD_10 = -8.3E+05
    
```

Figure 7 Preload Analysis of Gatimaan Express model.

The preload and linear analysis of model are shown in Figures 7 and 8. It is noted that preload on primary and secondary suspensions of the car bodies are identical. The model has negative real Eigen values after linear analysis which shows that the system is stable.

E I G E N V A L U E S at time = 0.00000E+00		
Number	Real (cycles/second)	Imag. (cycles/second)
1	0.00000E+00	
2	-5.97208E-02	
3	-6.10749E-02	
4	-6.10979E-02	
5	-6.27585E-02	
6	-6.27606E-02	
7	-6.29386E-02	
8	-6.35172E-02	
9	-6.38393E-02	
10	-6.41016E-02	
11	-6.41017E-02	
12	-6.50085E-02	
13	-6.50924E-02	
14	-6.50938E-02	
15	-6.51013E-02	
16	-6.51875E-02	
17	-6.51896E-02	
18	-6.55465E-02	
19	-6.55966E-02	
20	-6.58338E-02	
21	-6.59359E-02	
22	-6.62733E-02	
23	-6.63316E-02	
24	-6.65776E-02	
25	-6.66240E-02	
26	-6.66705E-02	
27	-6.73395E-02	
28	-6.73405E-02	
29	-6.73413E-02	

Figure 8 Linear Analysis of Gatimaan Express model.

The simulated results of lateral and vertical accelerations of model from VI-Rail are imported in Matlab/Simulink. They are further estimated through the Hammerstein-Wiener model to get best curve fit with the irrespective measured accelerations. It is shown that there is good match (85%) between the simulated results and measured sample data. The comparison of lateral and vertical accelerations are shown in Figures 9 and 10 respectively. The derailment of the model due to high speed (223 kmph) on the curve track is studied.

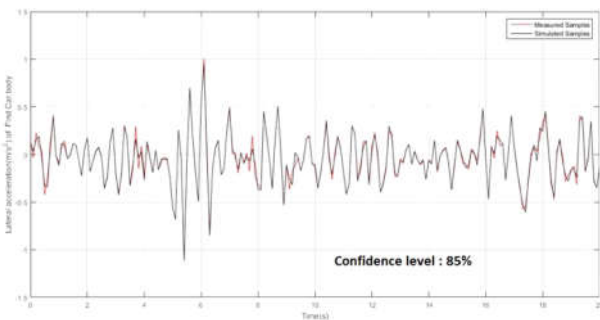


Figure 9 Comparison of Lateral Accelerations.

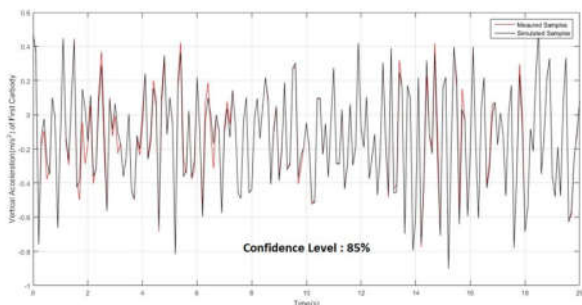


Figure 10 Comparison of Vertical Accelerations.

The critical speed is achieved after performing the simulation with various maximum speeds and is found that the derailment is occurred at 223 kmph. Nadal derived the following equation for derailment coefficient to avoid the flange climbing on the rail. The term (L/V) in the equation below is called derailment coefficient and it should be between 0.8-1 for railway vehicle to run safe [18]. Forces acting on wheel-rail contact is shown in Figure 11.

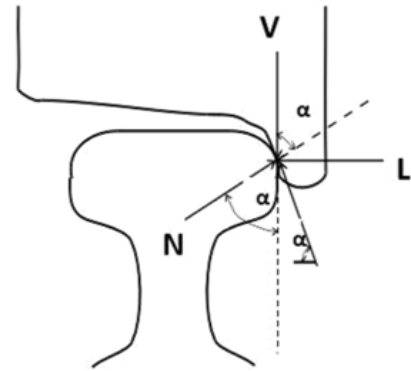


Figure 11 Forces acting on wheel-rail contact.

$$\frac{L}{V} \leq \frac{\tan \alpha - \mu}{(1 + \mu \tan \alpha)}, \tag{4}$$

Where  $\mu$ ,  $\alpha$ , L and V are the coefficient of friction of rail, flange angle, lateral wheel load and vertical wheel load respectively. The Figure 12 shows the derailment of 9<sup>th</sup> and 10<sup>th</sup> car bodies and the derailment coefficients of different car bodies are shown in Figure 13.

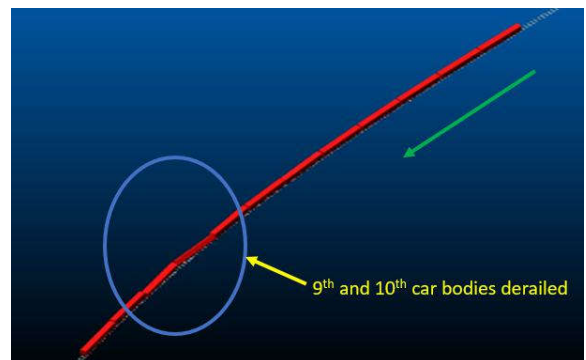


Figure 12 Derailment of Gatimaan Express model due to high speed.

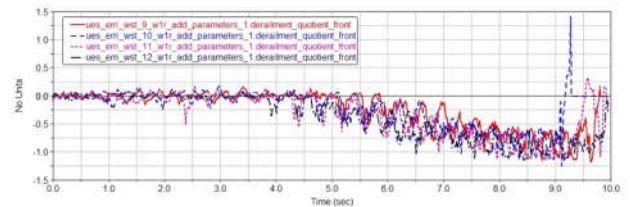


Figure 13 Derailment Coefficient of Gatimaan Express model due to high speed.

The derailment coefficient of 9<sup>th</sup> car body at about 9.2 seconds is about 1.4 which is higher than its limit 1 [19]. Centrifugal force ( $F_{cent}$ ) exerts torque (T) which tries to rotate the car body in clockwise direction about the wheel-rail contact at outer rail. At the same time, weight (W) of car body also exerts torque (load torque) which is in anticlockwise direction at the same time and encounters the torque (T) as shown in Figure 14.

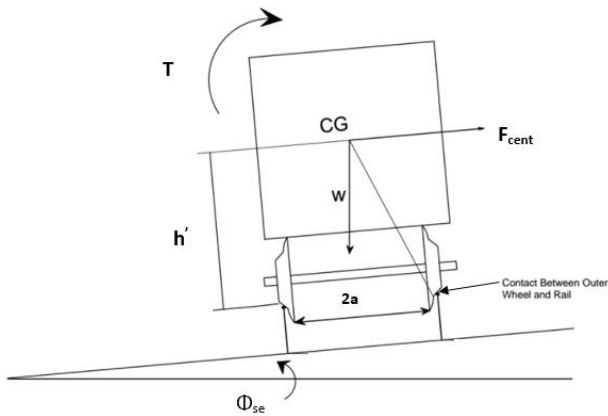


Figure 14 Train at the curve track.

If  $T$  is higher than load torque, derailment leads to occur because the lateral forces at that time becomes zero. The derailments due to failure of secondary and primary suspension are performed by altering the suspension parameter values in 12<sup>th</sup> car body, 6<sup>th</sup> car body and 1<sup>st</sup> car body as given in Table 2.

Table 2 Secondary and Primary Suspensions Spring Stiffness

Secondary Suspension Spring Stiffness (N/m)	base value	10% of base value
Longitudinal Spring Stiffness	10.0e06	10.0e05
Lateral Spring Stiffness	22.50e05	22.5e04
Vertical Spring Stiffness	35.0e05	35.0e04
Primary Suspension Spring Stiffness (N/m)	base value	10% of base value
Longitudinal Spring Stiffness	100.0e05	100.0e04
Lateral Spring Stiffness	250.0e06	250.0e05
Vertical Spring Stiffness	110.0e08	110.0e07

The derailment of 12<sup>th</sup> car body, 6<sup>th</sup> car body and 1<sup>st</sup> car body are shown in Figures 15, 17 and 19, and the respective derailment coefficients are shown in Figures 16, 18 and 20.

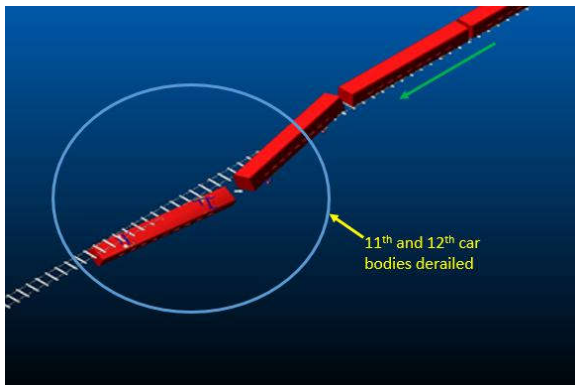


Figure 15 Derailment of 12<sup>th</sup> car body due to secondary suspension failure.

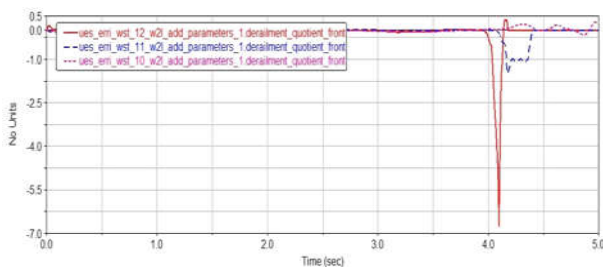


Figure 16 Derailment Coefficient of 12<sup>th</sup> car body due to secondary suspension failure.

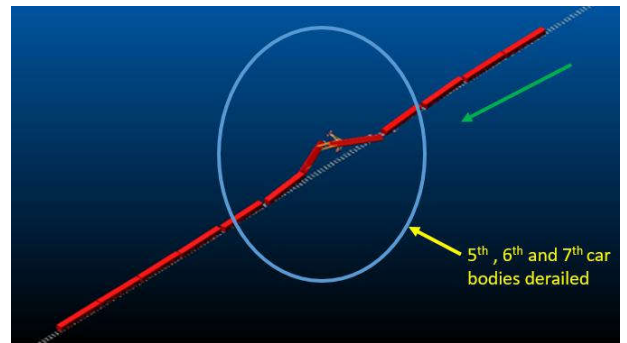


Figure 17 Derailment Coefficient of 6<sup>th</sup> car body due to secondary suspension failure.

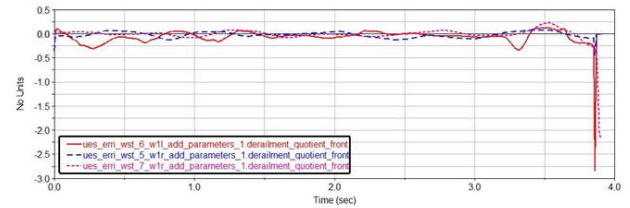


Figure 18 Derailment Coefficient of 6<sup>th</sup> car body due to secondary suspension failure.

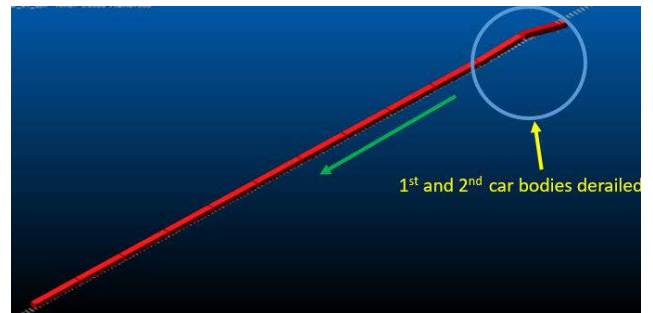


Figure 19 Derailment Coefficient of 1<sup>st</sup> car body due to secondary suspension failure.

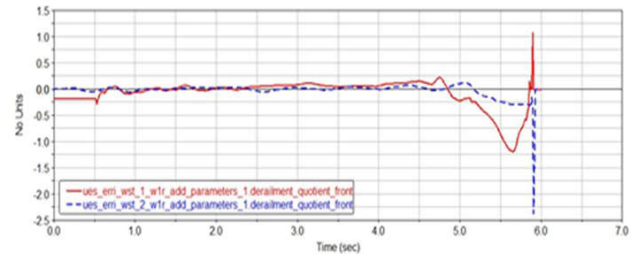


Figure 20 Derailment Coefficient of 1<sup>st</sup> car body due to secondary suspension failure.

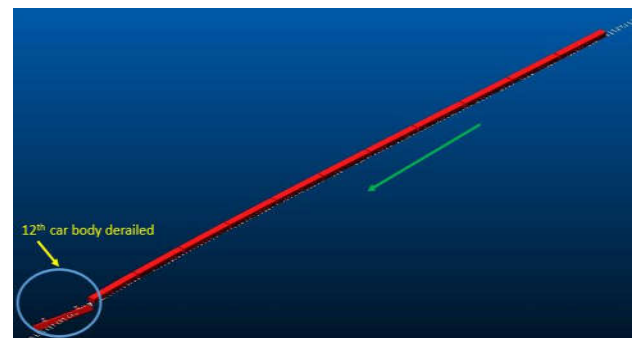


Figure 21 Derailment Coefficient of 12<sup>th</sup> car body due to primary suspension failure.

The 12<sup>th</sup>, 6<sup>th</sup>, 7<sup>th</sup>, 2<sup>nd</sup> and 1<sup>st</sup> car bodies are derailed due to failure of left primary suspensions are shown in Figures 21, 23, and 25.

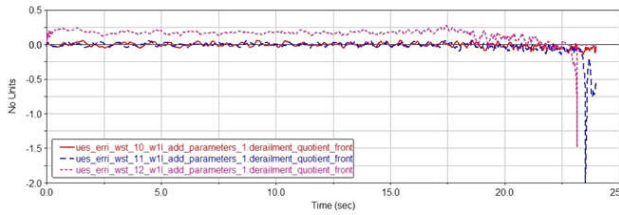


Figure 22 Derailment Coefficient of 12<sup>th</sup> car body due to primary suspension fail-ure.

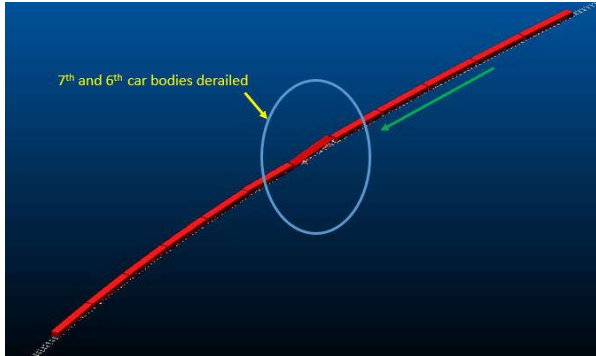


Figure 23 Derailment Coefficient of 6<sup>th</sup> car body due to primary suspension fail-ure.

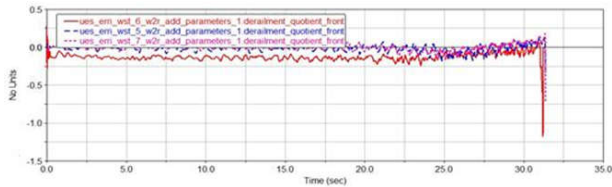


Figure 24 Derailment Coefficient of 6<sup>th</sup> car body due to primary suspension fail-ure.

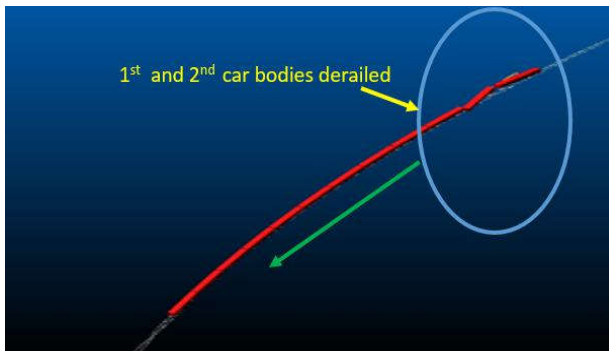


Figure 25 Derailment Coefficient of 1<sup>st</sup> car body due to primary suspension fail-ure.

The derailment quotients of respective car bodies in Figures 22, 24, and 26. It can be observed that derailments occur on the left secondary and primary suspensions. The input parameters used for this study are expressed in Table 3.

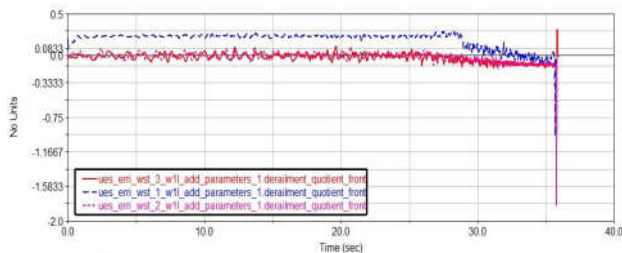


Figure 26 Derailment Coefficient of 1<sup>st</sup> car body due to primary suspension fail-ure.

Table 3 List of parameters assumed for simulation

Specification for car body	Specification for bogie	Specification for Wheelset
Mass of car body(kg) = 37740	Mass of bogie(kg) = 3000	Mass of Wheelset (kg) = 1600
Roll Inertia(kgm <sup>2</sup> ) = 56932	Roll Inertia(kgm <sup>2</sup> ) = 2120	Roll Inertia(kgm <sup>2</sup> ) = 1271
Pitch Inertia(kgm <sup>2</sup> ) = 1307220	Pitch Inertia(kgm <sup>2</sup> ) = 3206	Pitch Inertia(kgm <sup>2</sup> ) = 4763
Yaw Inertia(kgm <sup>2</sup> ) = 1309744	Yaw Inertia(kgm <sup>2</sup> ) = 5000	Yaw Inertia(kgm <sup>2</sup> ) = 1271
Secondary lat. damping rate(kNs=m) = 8500	Secondary vert. damping rate(kNs=m) = 7100	Primary vert. damping rate(kNs=m) = 4900
Series stiffness(kN=m) = 2150000	Series stiffness(kN=m) = 311000	Series stiffness(kN=m) = 2500000

## CONCLUSION AND REMARKS

1. The dynamics study of Gatimaan express model is successfully carried out. Simulated results and available experimental data with respect to lateral and vertical accelerations is in excellent agreement. The derailment coefficient at high speed crosses the Nadal limit (ratio of lateral to vertical force = 1). The derailment occurred due to increased inertial torque at the outer wheel and rail contact. This paper presents the dynamic performance of model based on the assumption that each car body is having same mass. The dynamic study can be more accurate if the load variation on each car body is considered.
2. Derailment due to failure of secondary and primary suspensions are studied. The objective of this study to understand the derailment due to suspension failure. Jinesh *et al.* [20] investigated the life time of suspension spring is 3-4 months. A mechatronics system can be installed on suspension to capture its online performance. When stiffness of the suspension crosses the threshold limit, warning for the replacement or maintenance of suspension is recorded.
3. This model can also be utilized to study for other upgradation of existing rail network. Performance of wear dynamics can be analyzed. Derailment due to failure of secondary and primary dampers can be investigated. It can be deployed to study the rail vehicle dynamics on account of the rail irregularities and track degradation due to excess traffic load.

This work is presented in VI Grade User's Conference in Wiesbaden, Germany dated on 11<sup>th</sup>-12<sup>th</sup>, April, 2016.

## Acknowledgment

The author would like to thank Testing Directorate and Track Machines and Monitoring Directorate, RDSO for providing the measured data during test run of Gatimaan Express and track geometry for New Delhi-Agra Cantonment Route.

## References

1. S. Sanjeev Arvind K., A. Ajit and R. Mukesh. Improvement in secondary suspension of ir20 coach using adams/rai. ADAMS/RAIL User's Conference, Germany, pp. 1-11, 2000.
2. A. Herrero. Towards optimization of a high speed train bogie primary suspension. Master's Thesis, Department

- of Applied Mechanics Division of Dynamics, Sweden, 2013.
3. K. Ellermann and M. Jesussek. Fault detection on isolation for nonlinear rail-way vehicle suspension system. 11th Int. Conference on Vibration Problems, Portugal, 2013.
  4. R. Melnik and Bogdan Sowiski. The selection procedure of diagnostic indicator of suspension fault modes for the rail vehicles monitoring system. 7th European Workshop on Structural Health Monitoring, France, pp.11–24, 2014.
  5. Bruni K. Bel Knani P. Bologna R. Lewis R.S. Dwyer-Joyce, A. Ward S and M. Cavalletti. Railway wheel wear predictions with adams/rail. ADAMS/RAIL User's Conference, 2010.
  6. M.R. Saat X. Liu and C.P.L. Barkan. Analysis of causes of major train derailment and their effect on accident rate. Transportation Research Board, pp. 154-163, 2012.
  7. S. W. Ju. Study of train derailment due to suspension damage. In Min-symposium on Interaction Dynamics of High Speed Railways, 11th World Congress on Computational Mechanics, Spain, 2014.
  8. Z. Lu and M. Hecht. Dynamic analysis of a new double deck passenger vehicle with bogie pw200. pp. 13-30, Istanbul, 2010.
  9. M. Montiglio and A. Stefanini. Development of a semi-active lateral suspension for a new titling train, 2012. <https://web.mscsoftware.com>.
  10. D. Thomas. Lateral stability of high-speed trains at unsteady crosswind. PhD Thesis KTH, Sweden, 2009.
  11. J. C. Moody. Critical speed analysis of railcars and wheelsets on curved and straight track. In Honor Thesis, Bates College, 2013.
  12. S. Sezer and A. Erdem Ataly. Dynamic modeling and fuzzy logic control of vibrations of a railway vehicle for different track irregularities. *Simulation Modelling Practice and Theory*, 19(1), pp.1873-1894, 2011.
  13. O. Polach. Creep forces in simulations of traction vehicles running on adhesion limit, Elsevier, Science Direct, 2004.
  14. Fan Y. Tsai and W. F. Wu. Stability analysis of railway vehicles and its verifications through field test data. *Journal of the Chinese Institute of Engineers*, 29:493-505, 2006.
  15. Reinhold Meisinger. Curving simulation and stability of a creep-controlled wheelset for high speed rail-vehicles. *Journal of the Brazilian Society of Mechanical Sciences*, 21(3), pp.493-505, 1999.
  16. Ministry of Railways Research Designs Standards Organization. Maintenance manual for BG coaches of LHB design. 2002.
  17. Vi-rail 15.0 documentation. 2013.
  18. Ministry of Railways Government of India. A technical guide on derailments. 1998.
  19. S. Iwnicki. Handbook of railway vehicle dynamics. pp. 256-266. CRC press, Taylor and Francis Group, Florida, 2006.
  20. G.S. Dangayach Jinesh K. J., M P. Singh and Dhananjay Chauhan. Smooth-ness running of train on uneven tracks with the help of air springs. *Inter-national Journal of Mechanical Engineering and Technology (IJMET)*, 5(9), pp.427-434, 2014.

**How to cite this article:**

Prabin Kumar Jha and Gokhale S.S. 2017, Modeling and Validation of Gatimaan Express with Vi-Rail. *Int J Recent Sci Res.* 8(11), pp. 21701-21707. DOI: <http://dx.doi.org/10.24327/ijrsr.2017.0811.1123>

\*\*\*\*\*